for $\varphi \in D_j \ (j=0,\ldots,n)$. It is known from the literature that (12) presents a good approximation to the exact yield surface.

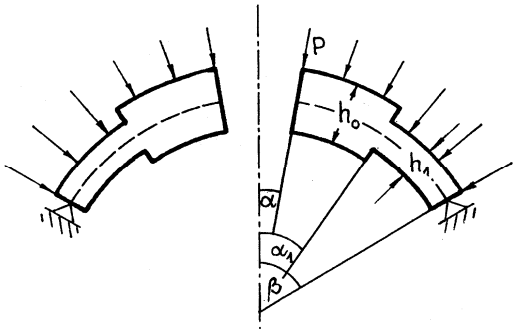

Fig.1. Spherical shell

According to the associated flow law and the yield surface (13) one has

$$\begin{aligned}
\varepsilon_1 &= \frac{\lambda_j(2N_1-N_2)}{N_{0j}^2}\\
\varepsilon_2 &= \frac{\lambda_j(2N_2-N_1)}{N_{0j}^2}\\
\kappa_1 &= \frac{\lambda_j(2M_1-M_2)}{M_{0j}^2}\\
\kappa_2 &= \frac{\lambda_j(2M_2-M_1)}{M_{0j}^2}
\end{aligned} \tag{14}$$

for $\varphi \in D_j \ (j=0,\ldots,n)$. Here λ_j stands for an unknown non-negative scalar multiplier. Evidently, equations (11) - (14) admit the presentation

$$\begin{aligned}
&N_1' = (N_2-N_1)\cot\varphi + Q\cot\varphi\\
&Q' = -N_1 - N_2 - P - Q\cot\varphi\\
&M_1' = (M_2-M_1)\cot\varphi + Q\\
&W' = Z\\
&U' = W + \frac{A\lambda_j}{N_{0j}^2}(2N_1-N_2)\\
&Z' = -W - \frac{A\lambda_j}{N_{0j}^2}(2N_1-N_2) - \frac{A^2\lambda_j}{M_{0j}^2}(2M_1-M_2)
\end{aligned} \tag{15}$$

and

$$\begin{aligned}
&Z + U + \frac{A^2\lambda_j}{\cot\varphi\, M_{0j}^2}(2M_2-M_1) = 0\\
&\frac{1}{A}(U\cot\varphi - W) - \frac{\lambda_j}{N_{0j}^2}(2N_2-N_1) = 0
\end{aligned} \tag{16}$$

for $\varphi \in D_j \ (j=0,\ldots,n)$.

From the system (16) one can define

$$\lambda_j = \frac{N_{oj}^2}{A(2N_2-N_1)}(U\cot\varphi - W), \tag{17}$$

provided $2N_2 \neq N_1$, and

$$\chi_j = Z + U + \frac{A\,N_{oj}^2}{M_{0j}^2\cot\varphi}\frac{2M_2-M_1}{2N_2-N_1}(U\cot\varphi - W) = 0 \tag{18}$$

for $j=0,\ldots,n$.

The material volume of the shell can be presented as

$$V = \sum_{j=0}^{n} h_j(\cos\alpha_j - \cos\alpha_{j+1}) \tag{19}$$

The minimum weight problem of the spherical cap is thus a particular case of (1) - (5) with $F_j = 0$, $G_j = h_j(\cos\alpha_j - \cos\alpha_{j+1})$ for $j=0,\ldots,n$. In this case $R_j = T_j = 0, A_0 = 0$ and $g_j = 0$. If the problem consists in the maximization of the limit load for given material volume (weight) of the shell then one has $G_0 = -P, \quad G_j = 0 \ (j=1,\ldots,n); F_j = 0$ and $T_j = h_j(\cos\alpha_j - \cos\alpha_{j+1})/(\alpha_{j+1} - \alpha_1)$ for $j=0,\ldots,n$ and $A_0 = V$.

6 Stepped conical shells

In the case of conical shells equilibrium equations have the form

$$\begin{aligned}
&(rN_1)' - N_2 = 0\\
&\left((rM_1)' - M_2\right)' - N_2\frac{\sin\varphi}{\cos^2\varphi} + \frac{Pr}{\cos^2\varphi} = 0
\end{aligned} \tag{20}$$

where prims denote differentiation with respect to the current radius and φ is the angle of inclination of a generator of the mid surface (Fig.2). Note that equations (20) can be obtained from (6) bearing in mind that φ = *const* and r_1 tends to infinity so that $dr = r_1\cos\varphi\, d\varphi$ remains finite.

The strain rate components corresponding to equations (20) are

$$\begin{aligned}
\varepsilon_1 &= \frac{dU}{dr}\cos\varphi\\
\varepsilon_2 &= \frac{1}{r}(U\cos\varphi + W\sin\varphi)\\
\kappa_1 &= -\frac{d^2W}{dr^2}\cos^2\varphi\\
\kappa_2 &= -\frac{1}{r}\frac{dW}{dr}\cos^2\varphi
\end{aligned} \tag{21}$$

It is assumed that the yield condition can be presented in this form (9) whereas the equation $\Phi_j = 0$ admits to determine

$$M_2 = M\left(M_1, N_1, N_2, M_{0j}, N_{0j}\right) \quad (22)$$
$$\text{for } r \in \left(a_j, a_{j+1}\right);\ j = 0, \ldots, n.$$

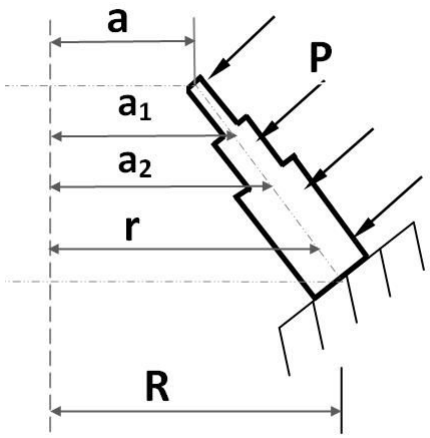

Fig. 2 Conical shell

It appears that the set of governing equations can be simplified, if one edge of the shell is absolutely free. Let us consider this case in the greater detail.
Substituting (22) in (20) and integrating the second equation with respect to *r* leads to the system

$$N_1' = \frac{1}{r}\left(N_2 - N_1\right)$$
$$M_1' = -\frac{1}{r}\left(M_1 - M\right) - N_1 \frac{\sin\varphi}{\cos^2\varphi} - \frac{P\left(r^2 - a^2\right)}{2\cos^2\varphi \cdot r} \quad (23)$$

where prims denote the differentiation with respect to *r*.

It can be easily rechecked that the associated flow law (10) with (21) yields

$$W' = Z$$
$$Z' = \frac{Z}{r\dfrac{\partial \Phi_j}{\partial M_2}} \cdot \frac{\partial \Phi_j}{\partial M_1} \quad (24)$$
$$U' = \frac{\lambda_j}{\cos\varphi} \cdot \frac{\partial \Phi_j}{\partial N_1}$$

and

$$W\sin\varphi + U\cos\varphi - r\lambda_j \frac{\partial \Phi_j}{\partial N_2} = 0 \quad (25)$$

whereas

$$\lambda_j = -\frac{Z\cos^2\varphi}{r} \frac{1}{\dfrac{\partial \Phi_j}{\partial M_2}} \quad (26)$$

$$\text{for } r \in \left(a_j, a_{j+1}\right);\ j = 0, \ldots, n.$$

Thus in the present case according to (23)-(26) one has five state variables $\left(N_1, M_1, W, Z, U\right)$ whereas in the general case the number of these is equal to six.

The material volume of a conical shell may be presented as

$$V = \frac{\pi}{\cos\varphi} \sum_{j=0}^{n} h_j \left(a_{j+1}^2 - a_j^2\right) \quad (27)$$

In (27) a_j stands for the radius of the circle separating parts of shells with thicknesses h_{j-1} and h_j, whereas $a_0 = a,\ a_{n+1} = R$

7 Stepped cylindrical shells

Let us consider small deflections of circular cylindrical shells of length *1* and radius *R* (Fig. 3). We shall confine our attention to axisymmetric free vibrations of the shell caused by an initial excitation.

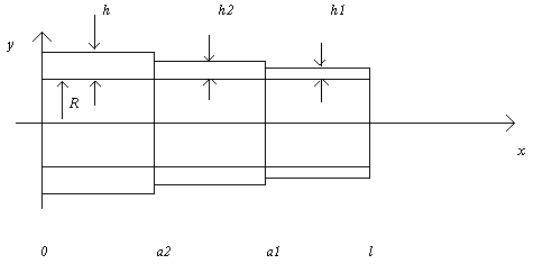

Fig.3: Stepped cylindrical shell

Let the origin of the axis *0x* be at the left end of the tube. Assume that the left end of the shell is clamped whereas the right hand end is absolutely free or simply supported. It is assumed that the thickness h of the shell is piece wise constant, e.g. $h(x) = h_j$ for $x \in \left(a_j, a_{j+1}\right)$, where $j = 0, \ldots, n$. Here the quantities $h_j\ (j = 0, \ldots, n)$ stand for fixed constants. Similarly, $a_j\ (j = 0, \ldots, n+1)$ are given constants whereas it is reasonable to use notations $a_0 = 0, a_{n+1} = 1$. It is known in the linear elastic fracture mechanics (see Anderson [2], Bronberg [5], Broek [6]) that repeated loading and stress concentration at sharp corners entail cracks. Thus it is reasonable to assume that at the re-entrant corners of steps e.g. at $x = a_j\ (j = 1, \ldots, n)$ cracks of depth c_j are located. For the simplicity sake we assume that these flaws are stable circular surface cracks. In the present study like Rizos *et al.* [33], Chondros *et al.* [11], Dimarogonos [13], Kukla [20] no attention will be paid to the crack extension during operation of the structure.

In the case of small deflections of axisymmetric cylindrical shells the stress resultants contributing to the strain energy are membrane forces N_1 and N_2 in axial and hoop direction, respectively, bending moment M and shear force Q. Equilibrium conditions of a shell element have the form (see Reddy [32], Soedel [34], Ventsel and Krauthammer [35])

$$\frac{\partial N_1}{\partial x} = \rho\, h_j \frac{\partial^2 U}{\partial t^2}$$
$$\frac{\partial M}{\partial x} = Q \qquad (28)$$
$$\frac{\partial Q}{\partial x} = \frac{N_2}{R} - p + \rho\, h_j \frac{\partial^2 W}{\partial t^2}$$

$x \in \left(a_j, a_{j+1}\right)$, where $j = 0,\ldots,n$. Here U and W stand for displacements in the axial and transverse direction whereas p is the intensity of distributed transverse pressure, ρ is the material density and t stands for time. Neglecting the axial force N_1 and the axial displacement U one can present the equilibrium equations (28) as

$$\frac{\partial^2 M}{\partial x^2} - \frac{N_2}{R} + p - \rho\, h_j \frac{\partial^2 W}{\partial t^2} = 0 \qquad (29)$$

for $x \in \left(a_j, a_{j+1}\right)$, $j = 0,\ldots,n$.

Strain components corresponding to the obtained equation of motion

$$\varepsilon_1 = \frac{\partial U}{\partial x}$$
$$\varepsilon_2 = \frac{W}{R} \qquad (30)$$
$$\kappa = -\frac{\partial^2 W}{\partial x^2}$$

It is assumed that in the case of shells made of isotropic elastic material generalized Hooke's law reads as (see Reddy [32])

$$\begin{Bmatrix} N_1 \\ N_2 \\ M \end{Bmatrix} = \frac{\mathrm{Eh}}{1-\nu^2} \begin{bmatrix} 1 & \nu & 0 \\ \nu & 1 & 0 \\ 0 & 0 & h^2/12 \end{bmatrix} \cdot \begin{Bmatrix} \varepsilon_1 \\ \varepsilon_2 \\ \kappa \end{Bmatrix} \qquad (31)$$

Substituting (31) with (30) in (29) yields the equation

$$\frac{\partial^4 W}{\partial x^4} + \frac{12\left(1-\nu^2\right)}{R^2 h_j^2} W = -\frac{12\rho\, h_j \left(1-\nu^2\right)}{E h_j^3} \frac{\partial^2 W}{\partial t^2} \qquad (32)$$

which must be satisfied for $x \in \left(a_j, a_{j+1}\right)$, $j = 0,\ldots,n$. When deriving (32) it was taken into account that according to the Hooke's law

$$N_1 = \frac{Eh}{1-\nu^2}\left(\varepsilon_1 + \nu\varepsilon_2\right)$$
$$N_2 = \frac{Eh}{1-\nu^2}\left(\nu\varepsilon_1 + \varepsilon_2\right)$$

Since $N_1 = 0$ and $\varepsilon_1 = -\nu\,\varepsilon_2$ one has

$$N_2 = Eh\frac{W}{R} \qquad (33)$$

and

$$\frac{\partial U}{\partial x} = -\nu\frac{W}{R} \qquad (34)$$

The presence of flaws or cracks in a structural member involves considerable local flexibilities. Additional local flexibility due to a crack depends on the crack geometry as well as on the geometry of the structural element and its loading. Probably the first attempt to prescribe the local flexibility of a cracked beam was undertaken by Irwin who recognized the relationship between the compliance C of the beam and stress intensity factor K. Later Dimarogonas [13]; Chondros *et al*. [10], Rizos *et al*. [33], Kukla [20] introduced so called massless rotating spring model which reveals the relationship between the stress intensity factor and local compliance of the beam. In the present paper we are following the papers by Chondros *et al*. [10] and assume that

$$W'\left(a_{j+},t\right) - W'\left(a_{j-},t\right) = \overline{C}_j\, M\left(a_j,t\right) \qquad (35)$$

where $\overline{C}_j$ stands for the additional compliance of the shell due to the crack.

The additional compliance $\overline{C}_j$ can be calculated making use of the methods of the linear elastic fracture mechanics (see Anderson [2], Lellep and Sakkov [28]).

It is easy to show that the equation of motion has a solution

$$W = \sin\omega t \cdot X_j(x)$$

for $x \in \left(a_j, a_{j+1}\right)$, $j = 0,\ldots,n$. It appears that

$$X_j(x) = A_j \sin\left(r_j x\right) + B_j \cos\left(r_j x\right) + C_j sh\left(r_j x\right) + D_j ch\left(r_j x\right)$$

where $A_j, B_j, C_j, D_j \ (j = 0,\ldots,n)$ are arbitrary constants. The constants of integrations are defined from the system of requirements including boundary and intermediate conditions (35). This leads to a linear homogeneous system of algebraic equations with the vanishing determinant Δ. From the equation $\Delta = 0$ one can calculate the characteristic numbers k_j versus crack lengths c_j.

8 Numerical results

The results of calculations are presented in Fig. 4 – Fig.11 and Table 1- 5.

In Table 1 optimal values of the design parameters are presented for the case of a spherical shell with a single step of the thickness. Table 1 corresponds to the maximization of the limit load for given weight of the spherical shell. Material of the shell obeys the yield

condition (13) with $j = 0$ and 1. Here γ stands for the ratio of thicknesses and $p = PA / N_*$, $N_* = 2\sigma_0 h_*$, σ_0 being the yield stress of the material. Here h_* is the thickness of the reference shell of constant thickness whereas p_* is the limit load for the reference shell. The coefficient of effectivity e is calculated as

$$e = \left(\frac{p}{p_*} - 1 \right) 100 .$$

Table 1: Optimal design of a spherical cap ($k=0,02$; $\alpha_0=0,8$; $\alpha_2=0,6$)

γ_0	α_1	γ_1	p	e
1,2	0,964	0,155	1,278	23,7%
1,4	0,938	0,176	1,398	35,4%
1,6	0,919	0,185	1,484	43,6%
1,8	0,904	0,199	1,545	49,5%
2,0	0,893	0,198	1,586	53,5%

It can be seen from Table 1 that the effectivity of the design is quite high even in the case of the design with single step of the thickness. When maximizing the limit load it is assumed that the optimized shell and the reference shell of constant thickness have the common weight.

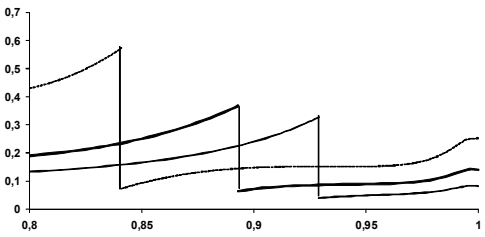

Fig. 4: Circumferential moment of spherical cap.

Calculations carried out showed that radial stress resultants N_1, M_1 are continuous at each point. However, N_2 and M_2 have jumps at these cross sections where the thickness has jumps. The distributions of the moment M_2 are presented in Fig.4. Here the bold, solid and dashed lines correspond to the ratios of thicknesses equal to 2.0, 4.0 and 1.5, respectively.

Calculations for stepped conical shells are implemented in the cases of the Mises' and Hill's yield conditions. Corresponding results are presented in Fig.5 and Table 2.

Fig.5 corresponds to the shell material which obeys the yield condition (13) and the associated flow law. In Fig.5 the nondimensional limit load of the conical shell versus α_1 is shown for different values of the ratio of thicknesses $h_1 / h_0 = \gamma_1$.

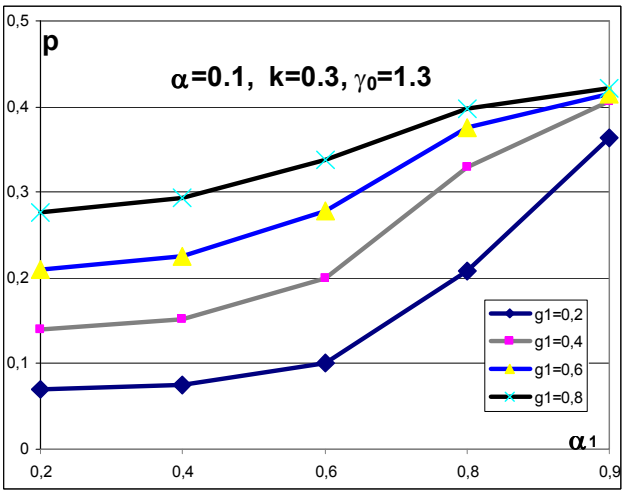

Fig. 5: Limit loads of conical shells.

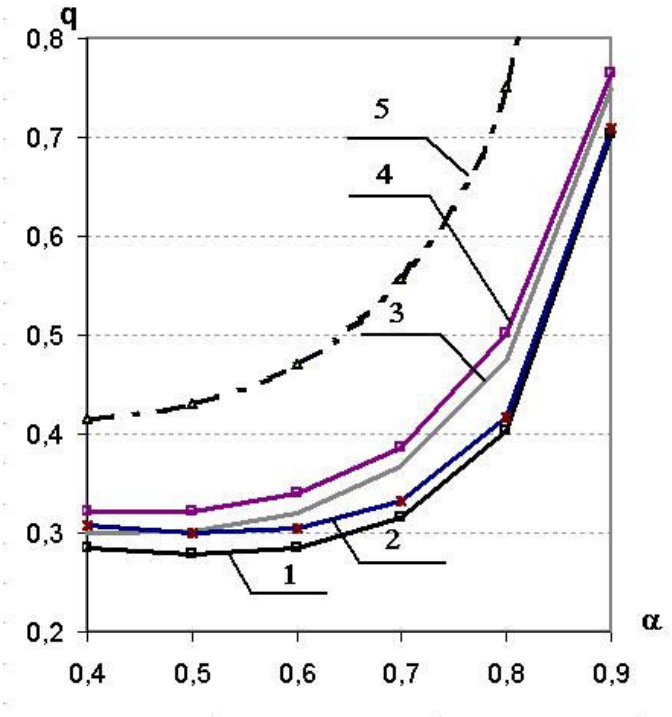

Fig. 6: Comparison with FEM.

Calculations have been carried out for the conical shell with the internal radius $a = 0,1R$ and $k = 0,3$ where the parameter

$$k = \frac{M_*}{RN_*} \frac{\cos^2 \varphi}{\sin^2 \varphi},$$

M_* being the limit moment of the reference shell with thickness h_*.

In Fig. 6 the solution procedure prescribed above is compared with the finite element method and the upper

bound solution. Here $k = 0.3$ and $q = P\sin\varphi$. The solutions obtained numerically by the finite element method are presented by curves 3 and 4. The finite element tehnique resorting to the beam element was implemented in Mathcad. In calculations about 100 elements were used. Curves 1 and 2 present the optimal solution of the problem with given upper bound of the thickness (here $h_0 / h_* = 1$ and $h_0 / h_* = 1.2$ respectively. The dashed line presents the upper bound solution for the shell of constant thickness.

The upper bound corresponds to the simpliest kinematically admissible distribution of velocities, whereas

$$W = W_0 \frac{r - R}{a - R}$$

Table 2: Optimal parameters of conical shells.

α_0	p	α_1	γ_0	γ_1	V_*	e
0,4	3,118	0,853	1,2	0,579	0,84	1,171
0,5	3,119	0,886	1,2	0,501	0,75	1,200
0,6	3,203	0,913	1,2	0,428	0,64	1,199
0,7	3,544	0,942	1,2	0,292	0,51	1,195
0,8	4,533	0,963	1,2	0,192	0,36	1,199

In Table 2 the first row shows the value of the internal radius of the shell whereas V_* is the material volume of the reference shell of constant thickness. Here $k = 0,3$.

Table 3: Optimal parameters of conical shells for $k = 0,5$ and $\gamma_0 = 1,3$.

α_0	P	P_0	γ_1	α_1	e
0,4	4,2489	3,8836	0,7519	0,7350	1,094
0,5	4,2803	3,9450	0,7039	0,7890	1,085
0,6	4,5114	4,2270	0,7184	0,8185	1,067
0,7	5,0983	4,9000	0,8194	0,8256	1,040
0,8	6,5570	6,4900	0,9524	0,8302	1,010
0,9	11,906	11,670	0,1409	0,9751	1,020

Optimal values of design parameters of conical shells made of a Hill's material are presented in Table 3. Table 3 corresponds to the problem of maximization of of the limit load. It can be seen from Tables 2 and 3 that in the case of conical shells the design with stepped thickness is more effective for shells with smaller values of k.

Results of calculations for elastic cylindrical shells clamped at the left end (Fig. 3) are presented in Fig.7-11 and Table 4-5. Free vibrations of stepped shells with cracks emanating at the re-entrant corners of steps are considered. Here $s = c / h$ stands for the ratio of the crack depth and shell wall thickness, respectively. In Fig.7 k is a characteristic number proportional to the natural frequency of the shell.

Curves 1-4 in Fig.7 correspond to different locations of steps indicated in Tables 4-5. The results presented herein correspond to shells with two steps located at $a_1 = \alpha_1 l$ and $a_2 = \alpha_1 l$, l being the half of length of the tube.

The tube under consideration has thicknesses $h_1 = 0,3h_0$ and $h_2 = 0,6h_0$.

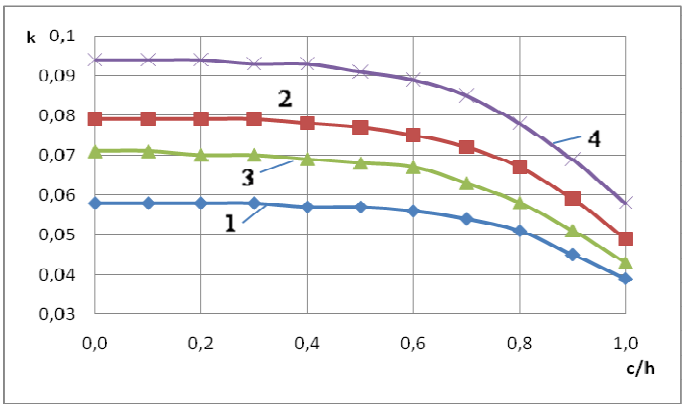

Fig. 7: Eigenfrequencies of the cracked shell.

Table 4: Eigenfrequencies of a cylindrical shell.

N	α_2	α_1	s=0,0	s=0,1	s=0,2	s=0,3	s=0,4	s=0,5
1	0,1	0,3	0,058	0,058	0,058	0,058	0,057	0,057
2	0,1	0,9	0,079	0,079	0,079	0,079	0,078	0,077
3	0,3	0,6	0,071	0,071	0,07	0,07	0,069	0,068
4	0,6	0,9	0,094	0,094	0,094	0,093	0,093	0,091

Table 5. Eigenfrequencies of a cylindrical shell.

N	α_2	α_1	s=0,6	s=0,7	s=0,8	s=0,9	s=1,0
1	0,1	0,3	0,056	0,054	0,051	0,045	0,039
2	0,1	0,9	0,075	0,072	0,067	0,059	0,049
3	0,3	0,6	0,067	0,063	0,058	0,051	0,043
4	0,6	0,9	0,089	0,085	0,078	0,069	0,058

It can be seen from Fig. 7 that the deeper the crack the lower the natural frequency of cracked shell. Fig. 8-9 correspond to the shell clamped at the left end and simply supported at the right hand end whereas results presented in Fig. 10-11 are associated with the tube with absolutely free right hand end. In Fig. 8 and Fig. 11 relationships between the characteristic number k and the crack length c/h are depicted for fixed locations of the step. Different curves in Fig.8 and Fig.11 correspond to different values of the ratio $\gamma = h_1 / h_0$. In Fig. 9 and Fig. 10 the ratio of thickness is fixed; different curves are associated with different locations of the step.

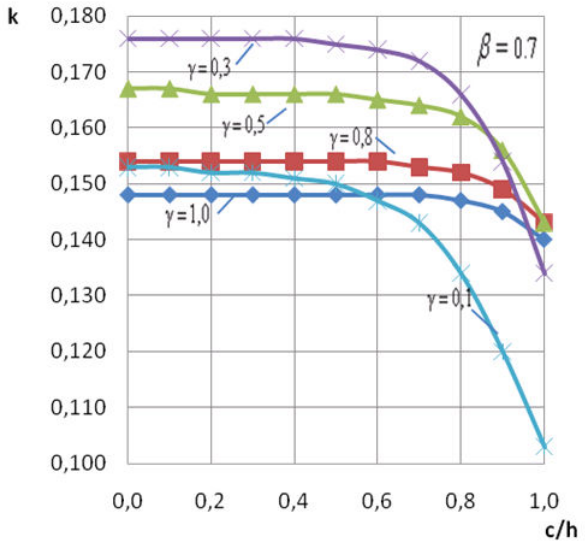

Fig. 8: Cantilever tube ($\beta = 0,7$)

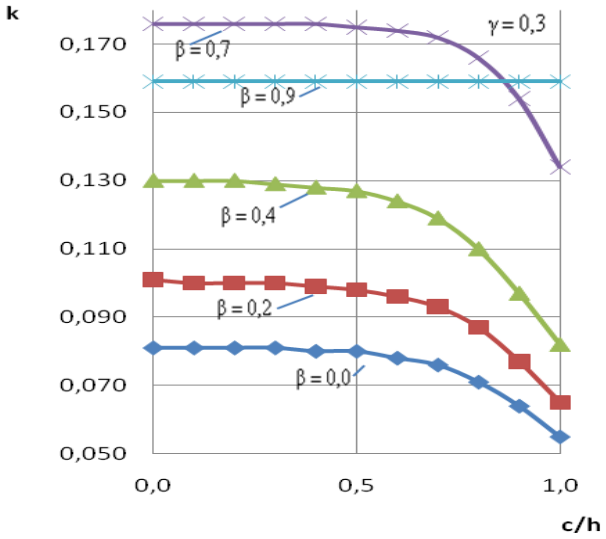

Fig. 9: Cantilever tube ($h_1 / h_0 = 0,3$)

9 Conclusion

Methods of optimization of both, elastic and inelastic shells were developed. Axisymmetric shells of piece wise constant thickness were considered. It was shown that the optimized shells were able to carry higher loads than corresponding reference shells of constant thickness. The cases of spherical, conical and circular cylindrical shells were studied in a greater detail. For spherical and conical shells made of materials which obey the Mises' and Hill's yield conditions the problems of minimum weight for constrained limit load and problems of maximum load carrying capacity for given weight have solved.

Calculations carried out showed that the load carrying capacity of spherical caps can be increased significantly even in the case of designs with one step of the thickness. When the number of steps is increased then the efficiency also increases. Similar conclusions can be drawn in the case of conical shells, as well.

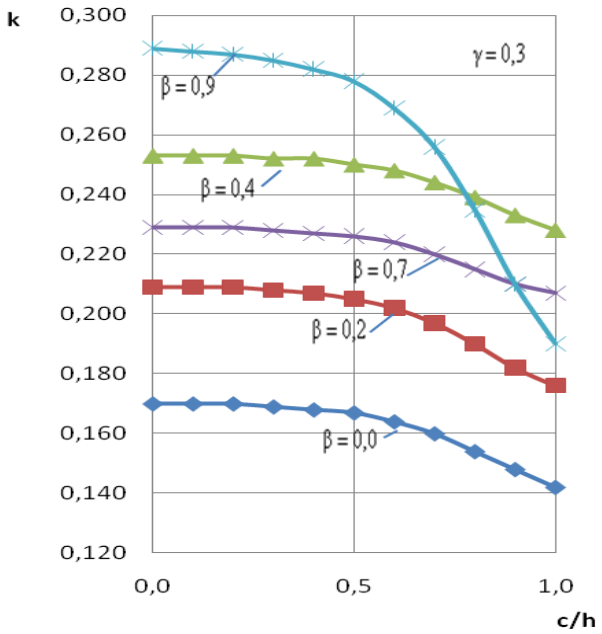

Fig. 10: Cracked tube ($h_1 / h_0 = 0,3$)

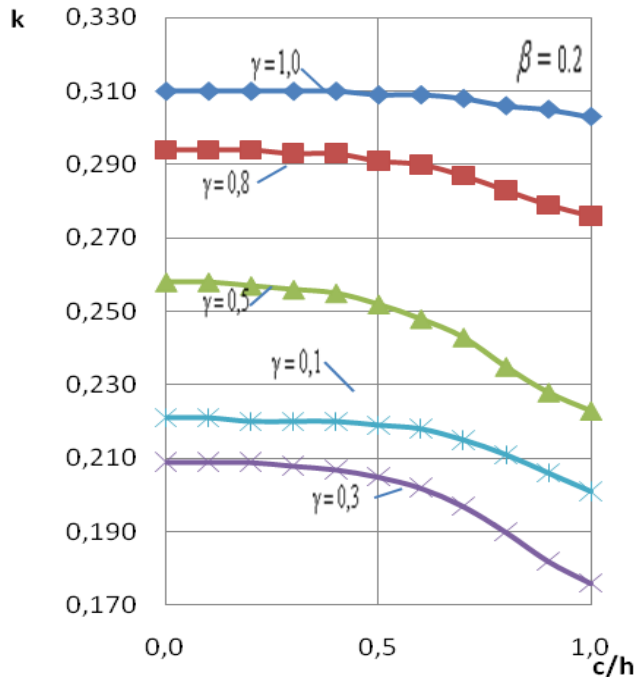

Fig. 11: Cracked tube ($a_1 / l = 0,2$)

Acknowledgement
The partial support of Estonian Science Foundation through the grant No 7461 is gratefully acknowledged.

References:

[1] N.U. Ahmed, *Dynamic Systems and Control with Applications*. World Scientific, New Jersey, 2006.
[2] T. Anderson, *Fracture Mechanics,* CRC Press, Boca Raton, 2005.
[3] N.V. Banichuk, *Introduction to Optimization of Structures*, Springer, Berlin, New York, 1990.
[4] M.P. Bendsoe, *Optimization of Structural Topology, Shape and Material*, Springer, Berlin, 1995.
[5] K.B. Broberg, *Cracks and Fracture,* Academic Press, New York, 1999.
[6] D. Broek, *The Practical Use of Fracture Mechanics,* Kluwer, Dordrecht, 1990.
[7] A. Bryson, Y.-C. Ho, *Applied Optimal Control*. Wiley, New York, 1975.
[8] A. Capsoni, L. Corradi, P. Vena, Limit analysis of orthotropic structures based on Hill's yield condition. *Int J. Solids Structures*, Vol. 38, 2001, pp. 3945-3963.
[9] J. Chakrabarty, *Applied Plasticity*, Springer-Verlag, New York, 2000.
[10] T.G. Chondros, A.D. Dimarogonas, J. Yao, A continuous cracked beam vibration theory, *J. Sound Vibr.,* Vol. 215, 1998, pp. 17-34.
[11] T.G. Chondros, A.D. Dimarogonas, J. Yao, Vibration of a beam with a breathing crack, *J. Sound Vibr.,* Vol. 239, 2001, pp. 57-67.
[12} L. Corradi, L. Luzzi, P. Vena, Finite element analysis of anisotropic structures. *Comput. Methods Appl. Mech. Engrg.,* Vol. 195, 2006, pp. 5422-5436.
[13] A.D. Dimarogonas, Vibration of cracked structures: a state of the art review. *Eng. Fracture Mech.,* Vol. 55, 1996, pp. 831-857.
[14] A.D. Dimarogonas, Buckling of rings and tubes with longitudinal cracks. *Mech. Res. Communic.,* Vol. 8, 1981, pp. 179-186.
[15] P. G. Hodge, *Limit Analysis of Rotationally Symmetric Shells*, Prentice Hall, New Jersey, 1963.
[16] D. G. Hull, *Optimal Control Theory for Applications*. Springer, Berlin, 2003.
[17] S. Kaliszky, J. Logo, Optimal design of elasto-plastic structures subjected to normal and extreme loads. *Computers and Structures*, Vol. 84 , 2006, pp. 1770 -1779.
[18] S. Kaliszky, J. Logo, Layout and shape optimization of elasto-plastic disks with bounds on deformation and displacement. *Mech. Struct. Mach.*, 30, 2002, pp. 177-192.
[19] U. Kirsch, *Structural Optimization; Fundamentals and Applications*. Springer, Berlin, 1993.
[20] S. Kukla, Free vibrations and stability of stepped columns, *J. Sound Vibr.,* Vol. 319, 2009, pp. 1301-1311.
[21] J. Krużelecki, M. Życzkowski, Optimal structural design of shells - A survey, *SM Archieves*, 10, 1985, pp. 101-170.
[22] D. Laplume, S. Datoussaid, G. Guerlement, Minimum weight design of solid annular plates under an assigned limit ring load, *Struct. Multidisc. Optimiz.*, Vol. 31, No.6, 2007, pp. 480-487.
[23] J. Lellep, Ü. Lepik, Analytical methods in plastic structural design, *Eng. Optimiz.*, Vol.7, No.3, 1984, pp. 209-239.
[24] J. Lellep, A. Mürk, Optimization of inelastic annular plates with cracks, *Struct. Multidisc. Optimiz.*, Vol.35, No.1, 2008, pp. 1-10.
[25] J. Lellep, E. Puman, Optimization of inelastic conical shells with cracks, *Struct. Multidisc. Optimiz.*, Vol.33, 2007, pp. 189-197.
[26] J. Lellep, E. Puman, Optimization of plastic conical shells of Mises material, *Struct. Multidisc. Optimiz.*, Vol.22, No.2, 2001, pp. 149-156.
[27] J. Lellep, E. Puman, Optimization of plastic conical shells loaded by a rigid central boss, *Int J. Solids Struct.*, Vol.37, 2000, pp. 2695-2708.
[28] J. Lellep, E. Sakkov, Buckling of composite columns, *Mech. Compos. Materials.*, Vol.42, 2006, pp. 63-72.
[29] J. Lellep, E. Tungel, Optimization of plastic spherical shells of Mises material, *Struct. Multidisc. Optimiz.*, Vol.30, No.5, 2005, pp. 381-387.
[30] J. Lellep, E. Tungel, Optimization of plastic spherical shells with a central hole, *Struct. Multidisc. Optimiz.*, Vol.23, No.3, 2002, pp. 233-240.
[31] L. Pan, R. Seshari, Limit analysis for anisotropic solids using variational principle and repeated finite element analysis. *Trans. CSME,* Vol. 28, 2004, pp. 89- 107.
[32] J.N. Reddy, *Theory and Analysis of elastic Plates,*CRC Press, Boca Raton, 2007.
[33] P.F. Rizos, N. Aspragathos, A.D. Dimarogonas, Identification of crack location and magnitude in a cantilever beam from the vibration modes, *J. Sound Vibr.,* Vol. 138, 1990, pp.381-388.
[34] W. Soedel, *Vibrations of Plates and Shells*, Marcel Dekker, New York, 2004.
[35] E. Ventsel, T. Krauthammer, *Thin Plates and Shells. Theory, Analysis and Applications*, Marcel Dekker, New York, 2001.